JAERI-Research
97-018

ANALYSIS OF DIVERTOR ASYMMETRY USING A SIMPLE FIVE-POINT MODEL

March 1997

Nobuhiko HAYASHI*, Tomonori TAKIZUKA
Akiyoshi HATAYAMA**and Masatada OGASAWARA**

日本原子力研究所
Japan Atomic Energy Research Institute

本レポートは，日本原子力研究所が不定期に公刊している研究報告書です。
入手の問合わせは，日本原子力研究所研究情報部研究情報課（〒319-11 茨城県那珂郡東海村）あて，お申し越しください。なお，このほかに財団法人原子力弘済会資料センター（〒319-11 茨城県那珂郡東海村日本原子力研究所内）で複写による実費頒布をおこなっております。

This report is issued irregularly.
Inquiries about availability of the reports should be addressed to Research Information Division, Department of Intellectual Resources, Japan Atomic Energy Research Institute, Tokai-mura, Naka-gun, Ibaraki-ken 319-11, Japan.

編集兼発行　日本原子力研究所
印　　刷　㈱原子力資料サービス

JAERI－Research 97－018

Analysis of Divertor Asymmetry Using a Simple Five-point Model

Nobuhiko HAYASHI*, Tomonori TAKIZUKA,
Akiyoshi HATAYAMA** and Masatada OGASAWARA**

Department of Fusion Plasma Research
Naka Fusion Research Establishment
Japan Atomic Energy Research Institute
Naka-machi, Naka-gun, Ibaraki-ken

(Received February 5, 1997)

A simple five-point model of the scrape-off layer (SOL) plasma outside the separatrix of a diverted tokamak has been developed to study the inside／outside divertor asymmetry. The SOL current, gas pumping／puffing in the divertor region, and divertor plate biasing are included in this model. Gas pumping／puffing and biasing are shown to control divertor asymmetry. In addition, the SOL current is found to form asymmetric solutions without external controls of gas pumping／puffing and biasing.

Keywords: SOL Plasma, Divertor, Tokamak, Divertor Asymmetry, SOL Current, Divertor Biasing, Gas Pumping／puffing, Divertor Modeling

*Fellow of Advanced Science (Keio University)
**Keio University

ダイバータ内外非対称性の簡易５点モデルによる解析

日本原子力研究所那珂研究所炉心プラズマ研究部
林　伸彦*・滝塚　知典・畑山　明聖**・小笠原正忠**

（1997年２月５日受理）

ダイバータ内外非対称性を解析するために，ダイバータ配位のトカマクにおけるスクレイプオフ層（SOL）を模擬した簡易５点モデルを開発した。このモデルは，SOL電流，ダイバータ領域におけるガス排気・注入，ダイバータバイアスの効果を取り入れている。ガス排気・注入およびダイバータバイアスによりダイバータ非対称性が制御できることが明らかになった。さらに，ガス排気・注入，ダイバータバイアスなどの外部制御がない場合でも，SOL電流が非対称なプラズマを形成することを示した。

那珂研究所：〒311-01　茨城県那珂郡那珂町向山801-1
＊特別研究生（慶應義塾大学）
＊＊慶應義塾大学

Contents

目　　次

1. Introduction

Inside/outside divertor asymmetry has been experimentally observed in several tokamaks with single-null divertor configuration[1-3]. Plasma densities, temperatures, heat fluxes, and so on, are different between inside and outside divertor plasmas. The asymmetry of the heat load on the divertor plates, i.e., too high heat load to the one-side plate, becomes the serious problem for the damage of the plates. On the other hand, the divertor asymmetry can be applied to the efficient removal of helium ash. When a tokamak reactor has only one pumping port, the control of the divertor asymmetry can make majority of ions from core plasma flow to the pumping side of the divertor.

The asymmetry is considered to be caused by the following reasons.

(a) Asymmetry of impurity radiation

(b) Asymmetry of neutral recycling

(c) Divertor biasing

(d) SOL current[3]

(e) Drift flow[4]

These effects for the analysis of the divertor asymmetry are essential.

Characteristics of divertor plasmas have been studied numerically. Among the numerical models of divertor plasmas, a two-point model is one of the simplest analytical model. This model clarified excellently the double-valued structures of the divertor plasma, i.e. low-recycling and high-recycling structures[5]. Two points mean the upstream-throat and the divertor plate. The model explains fairly well the results of the the experiments and complicated numerical simulations. It is convenient to use such a simple model for the simple representation of the divertor characteristics. The two-point model, however, is not enough for the analysis of the asymmetry, because it is difficult to include the effects mentioned above. In order to simulate the total SOL-divertor regions,

two two-point models need to be connected by putting a SOL plasma model between them. This combination of model is called a "five-point model".

In the present study, we develope a simple five-point model taking account of the effects causing the divertor asymmetry. The detailed description of the model is shown in the next section. Results of the analysis on the divertor asymmetry are demonstrated in section 3. Section 4 describes problems to be solved in future. Section 5 summarizes the key results of this work.

2. Simple five-point model

The SOL and divertor plasmas in a single-null divertor tokamak are schematically shown in Fig.1. Figure 2 shows a system used in the present five-point model, the region is divided into four regions i.e. two SOL regions and two divertor regions. The size of each region is measured along the magnetic field. Two divertor regions are in the separatrix legs under X-point and include sheath and pre-sheath near the divertor plates. Neutral recycling mainly occurs in these divertor regions. Two SOL regions are separated at a stagnation point where parallel ion flow velocity equals to zero. Ion flux, which diffuses out radially from core plasma, is divided at the stagnation point towards two divertor plates. Since few neutrals are ionized in the SOL, the diffusive ion flow is a main source of the parallel flux. In Fig.2, the left edge of the SOL connects the inside divertor A, and the right edge connects the outside divertor B. Fluid equations are integrated along a magnetic field line in each region and reduced a set of nonlinear equations with physical variables at the five positions, the left-side plate, left-side throat, stagnation point, right-side throat, and right-side plate. Accordingly we call the model used here a "simple five-point model". In this paper, we include the effects of neutral recycling, divertor biasing,

two two-point models need to be connected by putting a SOL plasma model between them. This combination of model is called a "five-point model".

In the present study, we develope a simple five-point model taking account of the effects causing the divertor asymmetry. The detailed description of the model is shown in the next section. Results of the analysis on the divertor asymmetry are demonstrated in section 3. Section 4 describes problems to be solved in future. Section 5 summarizes the key results of this work.

2. Simple five-point model

The SOL and divertor plasmas in a single-null divertor tokamak are schematically shown in Fig.1. Figure 2 shows a system used in the present five-point model, the region is divided into four regions i.e. two SOL regions and two divertor regions. The size of each region is measured along the magnetic field. Two divertor regions are in the separatrix legs under X-point and include sheath and pre-sheath near the divertor plates. Neutral recycling mainly occurs in these divertor regions. Two SOL regions are separated at a stagnation point where parallel ion flow velocity equals to zero. Ion flux, which diffuses out radially from core plasma, is divided at the stagnation point towards two divertor plates. Since few neutrals are ionized in the SOL, the diffusive ion flow is a main source of the parallel flux. In Fig.2, the left edge of the SOL connects the inside divertor A, and the right edge connects the outside divertor B. Fluid equations are integrated along a magnetic field line in each region and reduced a set of nonlinear equations with physical variables at the five positions, the left-side plate, left-side throat, stagnation point, right-side throat, and right-side plate. Accordingly we call the model used here a "simple five-point model". In this paper, we include the effects of neutral recycling, divertor biasing,

and SOL current to the model, but do not take account of the effects of impurity radiation and drift flow for simplicity. They should be introduced in future.

2.1 SOL model

We extend a two-point model[5] to include effects of plasma potential and SOL current. In this subsection, we explain a model to be applied to SOL regions shown in Fig.2. The model is based on the two-dimensional fluid equations i.e. particle, energy, generalized Ohm's law, and current equations, assuming that the electron temperature T_e and the ion temperature T_i are the same for simplicity, $T_e = T_i = T$.

$$\frac{\partial \Gamma}{\partial s} = -\frac{\partial}{\partial r}\Gamma_r = \frac{\partial}{\partial r}\left(D_\perp \frac{\partial n}{\partial r}\right) = S_{SOL} \tag{1}$$

$$\frac{\partial}{\partial s}(q + \phi j) = -\frac{\partial}{\partial r} q_r = \frac{\partial}{\partial r}\left(n\chi_\perp \frac{\partial T}{\partial r}\right) = W_{SOL} \tag{2}$$

$$\frac{\partial \phi}{\partial s} = -\frac{j}{\sigma} \tag{3}$$

$$\frac{\partial j}{\partial s} = 0 \tag{4}$$

where s is the length along the magnetic field, r is the radial length across the magnetic field. Quantities Γ, q, ϕ, j, and n, denote parallel flux of particle, parallel flux of energy, electric potential, SOL current density parallel to the magnetic field, and plasma density, respectively. The plasma pressure p is given by $p = nT$. The electric conductivity σ is a function of T, $\sigma = \sigma_0 T^{3/2}$. The particle diffusivity $D_\perp$, and the heat diffusivity $\chi_\perp$ are assumed constant for simplicity. Radial profiles of density and temperature are represented by e-folding lengthes λ_n, and λ_T, respectively,

$$n(s,r) = n(s)\exp\left(-\frac{r}{\lambda_n}\right) \tag{5}$$

$$T(s,r) = T(s)\exp\left(-\frac{r}{\lambda_T}\right). \tag{6}$$

The radial fluxes of particle and energy, Γ_r and q_r, from the core plasma to the SOL plasma can be written as[6],

$$\Gamma_r = \frac{D_\perp}{\lambda_n} n_0 \tag{7}$$

$$q_r = \frac{\chi_\perp}{\lambda_T} p_0 \tag{8}$$

where subscript 0 means the stagnation point. The source terms of particle and energy, S_{SOL} and W_{SOL}, in the SOL region are given by,

$$S_{SOL} = \frac{D_\perp}{\lambda_n{}^2} n_0 \tag{9}$$

$$W_{SOL} = \chi_\perp \left(\frac{1}{\lambda_T{}^2} + \frac{1}{\lambda_T \lambda_n}\right) p_0 . \tag{10}$$

Here a magnetic flux tube containing five points of the model is assumed to be the nearest one to the separatrix.

Two SOL regions are separated at the stagnation point. The length of the left-side SOL region along the magnetic field is expressed as $l_{stagnation}$, and that of the right-side SOL region is $L_{SOL} - l_{stagnation}$. The ion flux, which diffuses out radially from core plasma, is divided at that position towards two divertor plates. Integrating fluid equations, Eqs.(1)-(3), from the left edge of the SOL, which connects the divertor throat A, to the stagnation point, we derive the following simple equations.

$$\Gamma_{uA} = \int_0^{l_{stagnation}} S_{SOL} ds \tag{11}$$

$$q_0 + \phi_0 j = -q_{uA} + \phi_{uA} j + \int_0^{l_{stagnation}} W_{SOL} ds \tag{12}$$

$$\phi_0 - \phi_{uA} = -\frac{l_{stagnation}}{\sigma_0 T_0^{1.5}} j . \tag{13}$$

We also derive simple equations for the right side of the SOL,

$$\Gamma_{uB} = \int_{l_{stagnation}}^{L_{SOL}} S_{SOL} ds \tag{14}$$

$$q_{uB} + \phi_{uB} j = q_0 + \phi_0 j + \int_{l_{stagnation}}^{L_{SOL}} W_{SOL} ds \tag{15}$$

$$\phi_{uB} - \phi_0 = -\frac{L_{SOL} - l_{stagnation}}{\sigma_0 T_0^{1.5}} j. \tag{16}$$

The current j is constant along the magnetic field in accordance with Eq.(4).

2.2 Divertor model

In this subsection, we explain a model to be applied to divertor regions A and B shown in Fig.2. The system used here is illustrated in Fig.3. Basic equations of the model are the following one-dimensional fluid equations.

$$\frac{\partial \Gamma}{\partial s} = S_n \tag{17}$$

$$\frac{\partial}{\partial s}(q + \phi j) = W_n - P_{rad} \tag{18}$$

$$\frac{\partial \phi}{\partial s} = -\frac{j}{\sigma} + \frac{\alpha}{e}\frac{\partial T}{\partial s} + \frac{1}{en}\frac{\partial p}{\partial s} \tag{19}$$

$$\frac{\partial j}{\partial s} = 0 \tag{20}$$

where the thermal force coefficient α is given as $\alpha = 0.71$ for singly charged particles[7]. Radial diffusion in divertor regions are neglected unlike in SOL regions, because the source and sink terms in Eqs.(17) and (18) are much larger than diffusion terms.

The energy flux q includes both conductive and convective fluxes,

$$q = -\kappa_{e//}\frac{\partial T}{\partial s} - \left(\frac{5}{2} + \alpha\right)\frac{j}{e}T + 5T\Gamma, \tag{21}$$

where $\kappa_{e//} = \kappa_0 T^{5/2}$ is the electron heat conductivity parallel to the magnetic field. The difference between inside and outside electron temperatures can drive thermoelectric current[8]. The current also drives asymmetric parallel heat transport at a counter direction of the current as given by the second term in the R.H.S of Eq.(21)[9]. The parallel heat transport results in the electron temperature asymmetry.

The particle source and energy sink due to ionization of neutral particles are given by S_n and $W_n = -\Delta E \cdot S_n$, respectively, where ΔE denotes the ionization/excitation energy per an ionization event. Impurity radiation power P_{rad} plays an important role to cause detached divertor plasma. But in this study, since there is no exact evaluation of impurity radiation to use in the present model, only the ionization energy loss of deuterium ($\Delta E = 13.6eV$) is considered, $P_{rad} = 0$.

Integrating above equations from the upstream-throat of the divertor region to the plate, we derive a set of equations of a two-point model. Variables used here are shown in Fig.3. Note that these variables are in a magnetic flux tube near the separatrix, because their values at the upstream-throat connect those in the SOL region.

$$\Gamma_p - \Gamma_u = \int_0^{L_{div}} S_n ds \tag{22}$$

$$q_p + \phi_p j = q_u + \phi_u j - \Delta E \int_0^{L_{div}} S_n ds \tag{23}$$

$$\phi_s - \phi_u = -\frac{L_{div}}{\bar{\sigma}} j + \frac{\alpha}{e}\left(T_p - T_u\right) + \frac{1}{e\bar{n}}\left(n_p T_p - n_u T_u\right) \tag{24}$$

$$q_u = -\frac{2}{7}\kappa_0 \frac{T_p^{7/2} - T_u^{7/2}}{L_T} - \left(\frac{5}{2} + \alpha\right)\frac{j}{e} T_u + 5 T_u \Gamma_u \tag{25}$$

where L_{div} is the connection length between throat and plate along the magnetic field. The current j is constant along the magnetic field in accordance with Eq.(20). It is assumed that average density $\bar{n}$ is represented at throat density, and average electric conductivity $\bar{\sigma}$ is repersented at throat temperature i.e. $\bar{\sigma} \approx \sigma_0 T_u^{1.5}$. The characteristic length of temperature gradient L_T is assumed a distance from the stagnation point to the plate. Since the density and the temperature vary a little along the magnetic field in the SOL region for the attached divertor case, n_u and T_u are represented at stagnation point. Integrated source term in Eqs.(22) and (23) is modeled as follows[5],

$$\int_0^{L_{div}} S_n ds = \Gamma_p \left(1 - f_{pump}\right)\left\{1 - \exp\left(-\frac{\theta L_{div}}{\lambda}\right)\right\} \tag{26}$$

where the pitch of the magnetic field θ is much smaller than unity, and λ denotes the ionization mean-free-path of neutral particles, $\lambda = \upsilon_0 / n_p \langle \sigma\upsilon \rangle_{T_p}$. Thermal speed of neutrals $\upsilon_0 = \sqrt{T_p / m_0}$ and ionization rate coefficient $\langle \sigma\upsilon \rangle$ are evaluated at the plate. The gas pumping/puffing efficiency f_{pump} is defined as the ratio of pumping/puffing neutrals flux to that of neutralized ion flux at the plate. a positive value of f_{pump} corresponds to the case of pumping, while a negative value to the case of puffing.

Boundary conditions at the divertor plate are given on the basis of the sheath theory[10];

$$\Gamma_p = n_p \sqrt{\frac{2T_p}{m}} \tag{27}$$

$$\hat{j} = 1 - \exp\left\{\beta - \frac{e}{T_p}\left(\phi_s - \phi_p\right)\right\} \tag{28}$$

$$q_p = \gamma \Gamma_p T_p \tag{29}$$

$$\gamma = \gamma_0 - 2\hat{j} - \ln\left(1 - \hat{j}\right), \tag{30}$$

where $\hat{j}$ is the current density normalized by $e\Gamma_p$, γ is the heat transmission coefficient at the plate ($\beta = 2.8$, $\gamma_0 = 5.8$ for deutrium plasma). The sign of $\hat{j}$ is chosen positive when j flows into the plate, and is negative for outflowing current.

2.3 Pressure balance

Total (sum of ion and electron) momentum equation is written as follows

$$\frac{\partial}{\partial s}\left(mn\upsilon^2 + 2nT\right) = 0 \tag{31}$$

which dose not take account of the momentum loss. Integrating this equation from the stagnation point ($v=0$) to the inside divertor plate A and outside divertor plate B, respectively, we obtain

$$n_0 T_0 = 2n_{pA} T_{pA} = 2n_{pB} T_{pB}. \tag{32}$$

where the boundary condition Eq.(27) is used, $v_p \equiv \Gamma_p / n_p = \sqrt{2T_p/m}$. In detached plasma, the momentum loss becomes essential. We will discuss about this effect in section 4.

2.4 Numerical method

We give values of Γ_r, q_r, $D_\perp$, $\chi_\perp$, f_{pumpA}, f_{pumpB}, ϕ_{pA}, and ϕ_{pB}, as input parameters, and we obtain solutions, Γ_{pA}, Γ_{pB}, Γ_{uA}, Γ_{uB}, q_{pA}, q_{pB}, q_{uA}, q_{uB}, ϕ_{uA}, ϕ_{uB}, ϕ_{sA}, ϕ_{sB}, T_{pA}, T_{pB}, n_{pA}, n_{pB}, S_{nA}, S_{nB}, γ_A, γ_B, S_{SOL}, W_{SOL}, λ_n, λ_T, n_0, T_0, q_0, ϕ_0, j, and $l_{stagnation}$, to the set of 30 equations, Eqs.(7)-(16), (22)-(30), and (32). Note that Eqs.(22)-(30) are applied to the regions A and B, respectively. These nonlinear equations are solved by using a numerical method to find multiple solutions. This method is described in Appendix A.1.

3. Divertor asymmetry

Numerical calculations of divertor asymmetry have been carried out systematicaly using the five-point model described in the former section. The results are shown in this section. In sub-section 3.1, the divertor asymmetry caused by gas pumping/puffing is analized. The effect of the divertor biasing on the asymmetry is shown in sub-sections 3.2. Without controls of gas pumping/puffing and divertor biasing, divertor asymmetry induced by the SOL current is shown in sub-section 3.3.

Geometical parameters used in the model are $L_{SOL} = 78.0m$, $\theta \cdot L_{div} = 0.25m$, and $\theta = 0.075$, which are one of the typical parameters in JT-60U. Input parameters are $\Gamma_r = 1.1 \times 10^{20} m^{-2} s^{-1}$, $q_r = 1.0 \times 10^4 W/m^2$ (Total power across the separatrix is $1.2MW$), $D_\perp = 0.2\ m^2/s$, and $\chi_\perp = 10.0\ m^2/s$. Under these parameters, radial e-folding lengthes of density and temperature vary only a little, i.e., $\lambda_n = 3 \sim 4 \times 10^{-2} m$ and $\lambda_T = 1.4 \sim 2.0 \times 10^{-1} m$.

Divertor plasmas have two equilibrium states, as were found theoretically[5] and experimentally[3][11]. One is the high recycling state with high density and low temperature, and the other is the low recycling state with low density and high temperature. Nonlinear feature of the interaction between divertor plasma and neutral particles is the cause of this bi-stable solution. Under the above parameters, the divertor plasma practically has two equilibrium states mentioned above. In the present analysis, however, we treat only the case of the high recycling state. The low recycling state is considered to be not proper for the power and particle control in tokamak reactors.

3.1 Gas pumping/puffing

Effect of the gas pumping/puffing in divertor regions on the asymmetry is investigated. The gas pumping/puffing at outside diverotr

B is operated, while that at inside divertor A is not, i.e., f_{pumpA}=0. Biasing is not applied ($\phi_{pA} = \phi_{pB} = 0$) in this sub-section.

The gas pumping/puffing controls neutral recycling at outside divertor significantly. The flux amplification factor R defined by $R = \Gamma_p / \Gamma_u$ (see Fig.3) decreases significantly from 18 to 8 with the increase of f_{pumpB} from -0.1 to 0.1, as seen in Fig.4(a). The gas pumping/puffing also changes not only outside divertor plasma but also total SOL-divertors plasma. The stagnation point tends to shift toward higher recycling divertor and is decided by a equation derived from basic equations in the model,

$$\frac{l_{stagnation}}{L_{SOL}} = \frac{\Gamma_{uA}}{\Gamma_{uA} + \Gamma_{uB}} = \left(1 + R_A / R_B \left(T_{pA} / T_{pB} \right)^{\frac{1}{2}} \right)^{-1} \qquad (33)$$

depending on recycling factors and temperatures of both divertors.

Gas pumping makes outside neutral recycling decrease. Ions from core plasma flow more to the outside divertor than to the inside one (Fig.4(b)), i.e., the stagnation point shifts toward inside divertor. Ion flux at the outside divertor plate, however, is a little smaller than that at the inside divertor plate, since neutral recycling at outside is weaker than at inside. Plasma density at outside plate decreases and becomes lower than that at inside plate (Fig.4(c)). In contrast, plasma temperature at outside plate increases and becomes higher than that at outside plate because of the pressure balance along the magnetic field (Fig.4(d)). The temperature difference also causes a difference of sheath and presheath potentials between inside and outside divertor plasmas (thermoelectric effect[8]). A SOL current flows from outside to inside by the potential difference (Fig.4(e)).

The situations of gas pumping are illustrated in Fig.5(a). Key phenomena are summarized as follows.

1. Pumping at outside divertor.

2. Lower outside neutral recycling.

3. Decrement of plasma density and increment of temperature at outside plate.

4. Increment of presheath and sheath potentials at outside.

5. The SOL current flowing from outside to inside.

The SOL current carries the convective energy from inside to outside and amplifies the temperature difference between inside and outside. The SOL current destabilizes the equilibrium. However this instability is stabilized by the ion flow from core plasma. The ions from core plasma flow more to the outside than to the inside, and suppress the temperature difference. Therefore it is stable when the SOL current and the ion flow from core plasma have different directions each other, but unstable when they are in the same direction.

In the case of gas puffing, ions from core plasma flow more to the inside than to the outside. The stagnation point shifts toward outside. The same as gas pumping case, ion flux at outside divertor plate is a little larger than that at inside, since neutral recycling at outside is stronger than at inside. Neutral recycling tends to cancel change of ion flow from core plasma and balance plate fluxes between inside and outside in these situations. At last plasma density at outside plate increases and becomes higher than that at inside plate. In contrast, plasma temperature at outside plate decreases and becomes lower than that at inside plate. The temperature difference also causes a thermoelectric current towards outside.

The situations of gas puffing are illustrated in Fig.5(b). Key phenomena are summarized as follows.

1. Puffing at outside divertor.

2. Higher outside neutral recycling.

3. Increment of plasma density and decrement of temperature at outside plate.

4. Decrement of presheath and sheath potentials at outside.

5. The SOL current flowing from inside to outside.

The SOL current carries the convective energy from outside to inside and amplifies the temperature difference between inside and outside. The SOL current destabilizes the equilibrium. However this instability is stabilized by the ion flow from core plasma.

Figure.4(f) shows parallel heat fluxes at the throat and at the plate of each divertor. Heat flux at the throat is given by Eq.(25). Note the SOL current plays an important role to increase the difference between inside and outside throat heat fluxes. In the divertor regions, there are two causes which change the heat flow from the throat to the divertor plate. One is the ionization energy loss, and the other is heating or cooling due to the SOL current in sheath potential drop. The latter is explained as follows. The sheath potential drops toward the plate. The heating occurs as the current flows toward the plate, while the cooling occurs as it flows against the plate. This effect decreases the difference between inside and outside plate heat fluxes compared with the difference between inside and outside throat heat fluxes. In these gas pumping and puffing cases, the shift between inside and outside throat heat fluxes is larger than the heating and the cooling due to the SOL current.

The ionization energy loss reduces the total energy flow $W_{SOL}L_{SOL}$ by 24% without gas pumping/puffing. The total energy loss of ionization decreases from 27% to 18% with increase of f_{pumpB} from -0.1 to 0.1. Especially the outside divertor part of the ionization loss decreases from 15% to 7%. In contrast, the inside part decreases a little.

In the case of the gas pumping, the cooling due to the SOL current occurs in the outside divertor region and the heating occurs in the inside. The cooling and the heating have almost the same amount and reach about 8% of the total energy flow for $f_{pumpB} = 0.1$. This effect

compensates the decrease of ionization energy loss at outside and cancels the ionization energy loss at inside with increase of f_{pumpB}. The shift between inside and outside throat heat fluxes which reachs about 12% of the total energy flow for $f_{pumpB}=0.1$ is modified by these effects in divertor regions. At last, gas pumping makes heat flux at outside divertor plate increase while heat flux at inside plate is almost constant, as seen in Fig.4(f).

On the other hand, gas puffing makes heat flux at outside plate decrease while heat flux at inside plate is almost constant. The heating due to the SOL current occurs in the outside divertor region and the cooling occurs in inside. The heating and the cooling have almost the same amount and reach about 4% of the total energy flow for $f_{pumpB}=-0.1$. This effect cancels the increase of ionization energy loss at outside and adds the ionization energy loss at inside with decrease of f_{pumpB}. The shift between inside and outside throat heat fluxes which reachs about 6% of the total energy flow for $f_{pumpB}=-0.1$ is modified by these effects in divertor regions.

3.2 Divertor biasing

Effects of the divertor biasing on the asymmetry is investigated. The divertor plates is electrically biased between the inside and the outside divertor plates ($\phi_{pB}-\phi_{pA}=V$). Gas pumping and puffing are not applied ($f_{pumpA}=f_{pumpB}=0$). The solution without biasing is symmetric.

Biasing causes the asymmetry so that ions from core plasma flow to prevent external biasing potential given at the plate to penerate into center SOL region. Positive biasing makes ions from core plasma flow more to the outside divertor than to the inside one (Fig.6(b)). The stagnation point shifts toward inside. Plasma density increases and temperature decreases at outside plate, while density decreases and

temperature increases at inside plate (Fig.6(c)(d)). Potential drop of outside sheath decreases and that of inside increases according to each temperature. At last potential drop in center SOL region is smaller than the external biasing potential. A current which responds to the potential drop flows from outside to inside (Fig.6(e)). These situations are the same as the case of negative biasing.

Figure.6(f) shows parallel heat fluxes at the throat and at the plate of each divertor. The SOL current plays an important role to increase the difference between inside and outside throat heat fluxes. However the relation of throat heat flux between inside and outside divertors is reversed at the plate. As positive biasing increases, the throat heat flux at outside becomes larger than that at inside, but the plate heat flux at outside becomes smaller than that at inside. It is the heating or the cooling due to the SOL current in sheath potential drop that causes the reversal. The ionization energy losses of each divertor are almost constant 12% of the total energy flow with any biasing. In this biasing case, the shift between inside and outside throat heat fluxes which reachs about 5% of the total energy flow for $eV/T_0 = 0.4$ is smaller than the heating and the cooling due to the SOL current which have almost the same amount of about 10%. The heating and the cooling cancel and exceed the shift. The former is doninant to change plate heat fluxes in these biasing cases. These changes of plate heat flux also cause the changes of each plate temperature mentioned above.

Figure.6(a) shows dependence of neutral recycling on biasing. Neutral recycling increases with the plate temperature because the rate coefficient of ionization increases with temperature in low temperature regime. In positive biasing, inside recycling increases and outside recycling decreases depending on each plate temperature. Neutral recycling tends to weaken change of ion flow from core plasma as seen in plate fluxes of Fig.6(b). This tendency is the same as the gas

pumping/puffing asymmetry. In positive biasing, inside neutral recycling is stronger than outside, while particle flux at inside throat is smaller than that at outside throat. So the difference of flux at plate is smaller than that at throat. These changes also cause the shift of the stagnation point explained by Eq.(33).

The situations of the positive biasing explained above are illustrated in Fig.7. Key phenomena are summarized as follows.

1. Positive biasing.
2. The SOL current flowing from outside to inside.
3. The cooling due to the SOL current in outside divertor region, and the heating at inside.
4. Increment of plasma density and decrement of temperature at outside plate. Decrement of density and increment of temperature at inside plate.
5. Lower recycling at outside, and higher recycling at inside.
6. Larger ion flow to the outside throat.

The SOL current carries the convective energy from inside to outside and reduces the temperature difference between inside and outside. The SOL current stabilizes the equilibrium.

3.3 SOL current induced asymmetry

Without controls of gas pumping/puffing and biasing, i.e., $f_{pumpA} = f_{pumpB} = 0$ and $\phi_{pA} = \phi_{pB} = 0$, two asymmetric solutions induced by SOL current have been found in addition to a symmetric solution. Input parameters are the same as those in previous sub-sections except for the particle flow from the core plasma Γ_r.

One solution has a current towards outside, and the other has a current towards inside. No current solution is symmetric. The two asymmetric solutions are reverse each other with the symmetric solution. The situation of gas pumping/puffing and biasing mentioned in

previous sections has only a symmetric solution without controls because of the smaller particle flow from core plasma.

The asymmetric solutions form the SOL current self-consistently. In the case of the current towards outside, convective energy is carried from outside to inside by the current (Fig.8(f)). Since inside plate temperature increases and outside one decreases (Fig.8(e)), plasma density at outside plate becomes higher than that at inside plate (Fig.8(d)). Potential drop of outside sheath decreases and that of inside increases according to each temperature. Electric field towards outside sustains the SOL current. Fig.8(a) shows neutral recycling increases at inside and decreases at outside depending on each plate temperature. These changes also cause the shift of the stagnation point explained by Eq.(33). The stagnation point shifts toward inside. Ions from core flow more to the outside divertor than to the inside one (Fig.8(c)). This is the same as the current towards inside.

Figure.8(f) shows heat fluxes at the throat and at the plate of each divertor. The SOL current plays an important role to increase the difference between inside and outside throat heat fluxes. The ionization energy losses of each divertor are almost constant 14% of the total energy flow with any current. In this case, the shift between inside and outside throat heat fluxes is larger than the heating and the cooling due to the SOL current. For example, the shift between inside and outside throat heat fluxes reachs about 10% of the total energy flow when j/enCs equals 0.1, while the heating and the cooling have almost the same amount of about 5%. The heating and the cooling weaken the shift between inside and outside throat heat fluxes.

The situations of the current towards outside explained above are illustrated in Fig.9. Key phenomena are summarized as follows.

1. The SOL current flowing from inside to outside.

2. The energy shift by the SOL current from outside to inside.

3. Increment of plasma density and decrement of temperature at outside plate. Decrement of plasma density and increment of temperature at inside plate.
4. Electric field towards outside sustaining the SOL current.
5. Lower recycling at outside, higher recycling at inside.
6. Larger ion flow to the outside throat.

In these asymmetries induced by the SOL current, the values of the particle flow from core plasma are larger than that of the situation of gas pumping/puffing and biasing mentioned in previous sections. The convective energy of the ion flow plays an important role to reduce the temperature difference caused by the current. Differently from the cases in previous sections, the energy of the ion flow from core plasma stabilizes the equilibrium.

The model includes only SOL-divertor plasmas. The SOL current flows along the magnetic field line in plasma, injects into the plate, passes through conducting wall and comes back to plasma at the opposite plate. The conductivity of the wall can affect the equilibrium in plasma. It will be necessary to take account of the wall in order to study the asymmetry.

4. Discussion

In the present model, there are many assumptions and problems, as summarized below. They will be solved as future works.

4.1 Neutral

Neutral model in this model was so simple that it could not represent any low neutral recycling situations quantitatively. More detail model should be used to study inside/outside divertor asymmetry caused by the combination of high and low neutral recyclings in divertor regions.

3. Increment of plasma density and decrement of temperature at outside plate. Decrement of plasma density and increment of temperature at inside plate.
4. Electric field towards outside sustaining the SOL current.
5. Lower recycling at outside, higher recycling at inside.
6. Larger ion flow to the outside throat.

In these asymmetries induced by the SOL current, the values of the particle flow from core plasma are larger than that of the situation of gas pumping/puffing and biasing mentioned in previous sections. The convective energy of the ion flow plays an important role to reduce the temperature difference caused by the current. Differently from the cases in previous sections, the energy of the ion flow from core plasma stabilizes the equilibrium.

The model includes only SOL-divertor plasmas. The SOL current flows along the magnetic field line in plasma, injects into the plate, passes through conducting wall and comes back to plasma at the opposite plate. The conductivity of the wall can affect the equilibrium in plasma. It will be necessary to take account of the wall in order to study the asymmetry.

4. Discussion

In the present model, there are many assumptions and problems, as summarized below. They will be solved as future works.

4.1 Neutral

Neutral model in this model was so simple that it could not represent any low neutral recycling situations quantitatively. More detail model should be used to study inside/outside divertor asymmetry caused by the combination of high and low neutral recyclings in divertor regions.

4.2 Impurity radiation

This model dose not take account of the energy loss by impurity radiation. Importance of impurity radiation, however, has been reported from many divertor experiments. Different amounts of impurity radiation loss between inside and outside divertor regions are the one of the major causes of the divertor asymmetry. The divertor model should take account of it especially for the high neutral recycling regime.

4.3 Momentum loss

Plasma pressure is conserved along the magnetic field line as given by Eq.(32) in the case of low neutral recycling. On the other hand, the pressure drops towards the plate through momentum loss by plasma-neutral interactions (elastic collision, charge exchange and so on) in cases of high recycling and detached plasmas. The effect of momentum loss on the divertor asymmetry will be also introduced to the model.

4.4 Drift flow

There are three kinds of drift flow in the SOL, i.e., $E \times B$, diamagnetic, and ∇B drifts. A drift flow towards inside or outside divertor also causes the divertor asymmetry. Dependences of the divertor asymmetry on drift flows have been reported from many divertor experiments. The effects of those drifts on the divertor asymmetry will be studied in the future.

Other asymmetries, such as asymmetric source due to anomalous diffusion, will be also studied.

5. Summary

A simple five-point model of the scrape-off layer outside the separatrix of a diverted tokamak plasma has been developed to study inside/outside divertor asymmetry. Gas pumping/puffing and biasing are shown to control the divertor asymmetry. In addition, the SOL current is found to form asymmetric solutions without external controls of gas pumping/puffing and biasing.

The results in this paper are restricted for the small range of the input parameters. Parametric dependence of characteristics of the SOL and divertor plasmas will be reported in the future.

Acknowledgments

One of the authors(N.H) would like to thank Drs. T. Hirayama, H. Shirai, N. Asakura, K. Shimizu, and A. Sakasai for their discussions, supports and encouragements during his stay in JAERI as a fellow of advanced science.

References

[1] T.Shoji et al., J. Nucl. Mater. **220-222**(1995)357.

[2] N.Asakura et al., 15th IAEA Conf.(Seville,1994).

[3] B.LaBombard et al., 12th PSI Conf.(San Raphael, 1996)

[4] P.C.Stangeby et al., Nucl. Fusion **36**(1996)839.

[5] M.Sugihara et al., J. Nucl. Mater.**128-129**(1984)114.

[6] T.Takizuka, J. Plasma and Fusion Research **64**(1990)255.

[7] S.I.Braginskij, in Reviews of Plasma Physics, Vol.1 (M.A.Leontovich,Ed.), Consultants Bureau, New York (1966)205.

[8] G.M.Staebler, Nucl. Fusion **29**(1989)1820.

[9] M.J.Schaffer et al., J. Nucl. Fusion **32**(1992)855.

[10] G.M.Staebler, Nucl. Fusion **31**(1991)729.

[11] K.Shimizu et al., J. Nucl. Mater. **196-198**(1992)476.

5. Summary

A simple five-point model of the scrape-off layer outside the separatrix of a diverted tokamak plasma has been developed to study inside/outside divertor asymmetry. Gas pumping/puffing and biasing are shown to control the divertor asymmetry. In addition, the SOL current is found to form asymmetric solutions without external controls of gas pumping/puffing and biasing.

The results in this paper are restricted for the small range of the input parameters. Parametric dependence of characteristics of the SOL and divertor plasmas will be reported in the future.

Acknowledgments

One of the authors(N.H) would like to thank Drs. T. Hirayama, H. Shirai, N. Asakura, K. Shimizu, and A. Sakasai for their discussions, supports and encouragements during his stay in JAERI as a fellow of advanced science.

References

[1] T.Shoji et al., J. Nucl. Mater. **220-222**(1995)357.

[2] N.Asakura et al., 15th IAEA Conf.(Seville,1994).

[3] B.LaBombard et al., 12th PSI Conf.(San Raphael, 1996)

[4] P.C.Stangeby et al., Nucl. Fusion **36**(1996)839.

[5] M.Sugihara et al., J. Nucl. Mater.**128-129**(1984)114.

[6] T.Takizuka, J. Plasma and Fusion Research **64**(1990)255.

[7] S.I.Braginskij, in Reviews of Plasma Physics, Vol.1 (M.A.Leontovich,Ed.), Consultants Bureau, New York (1966)205.

[8] G.M.Staebler, Nucl. Fusion **29**(1989)1820.

[9] M.J.Schaffer et al., J. Nucl. Fusion **32**(1992)855.

[10] G.M.Staebler, Nucl. Fusion **31**(1991)729.

[11] K.Shimizu et al., J. Nucl. Mater. **196-198**(1992)476.

5. Summary

A simple five-point model of the scrape-off layer outside the separatrix of a diverted tokamak plasma has been developed to study inside/outside divertor asymmetry. Gas pumping/puffing and biasing are shown to control the divertor asymmetry. In addition, the SOL current is found to form asymmetric solutions without external controls of gas pumping/puffing and biasing.

The results in this paper are restricted for the small range of the input parameters. Parametric dependence of characteristics of the SOL and divertor plasmas will be reported in the future.

Acknowledgments

One of the authors(N.H) would like to thank Drs. T. Hirayama, H. Shirai, N. Asakura, K. Shimizu, and A. Sakasai for their discussions, supports and encouragements during his stay in JAERI as a fellow of advanced science.

References

[1] T.Shoji et al., J. Nucl. Mater. **220-222**(1995)357.

[2] N.Asakura et al., 15th IAEA Conf.(Seville,1994).

[3] B.LaBombard et al., 12th PSI Conf.(San Raphael, 1996)

[4] P.C.Stangeby et al., Nucl. Fusion **36**(1996)839.

[5] M.Sugihara et al., J. Nucl. Mater.**128-129**(1984)114.

[6] T.Takizuka, J. Plasma and Fusion Research **64**(1990)255.

[7] S.I.Braginskij, in Reviews of Plasma Physics, Vol.1 (M.A.Leontovich,Ed.), Consultants Bureau, New York (1966)205.

[8] G.M.Staebler, Nucl. Fusion **29**(1989)1820.

[9] M.J.Schaffer et al., J. Nucl. Fusion **32**(1992)855.

[10] G.M.Staebler, Nucl. Fusion **31**(1991)729.

[11] K.Shimizu et al., J. Nucl. Mater. **196-198**(1992)476.

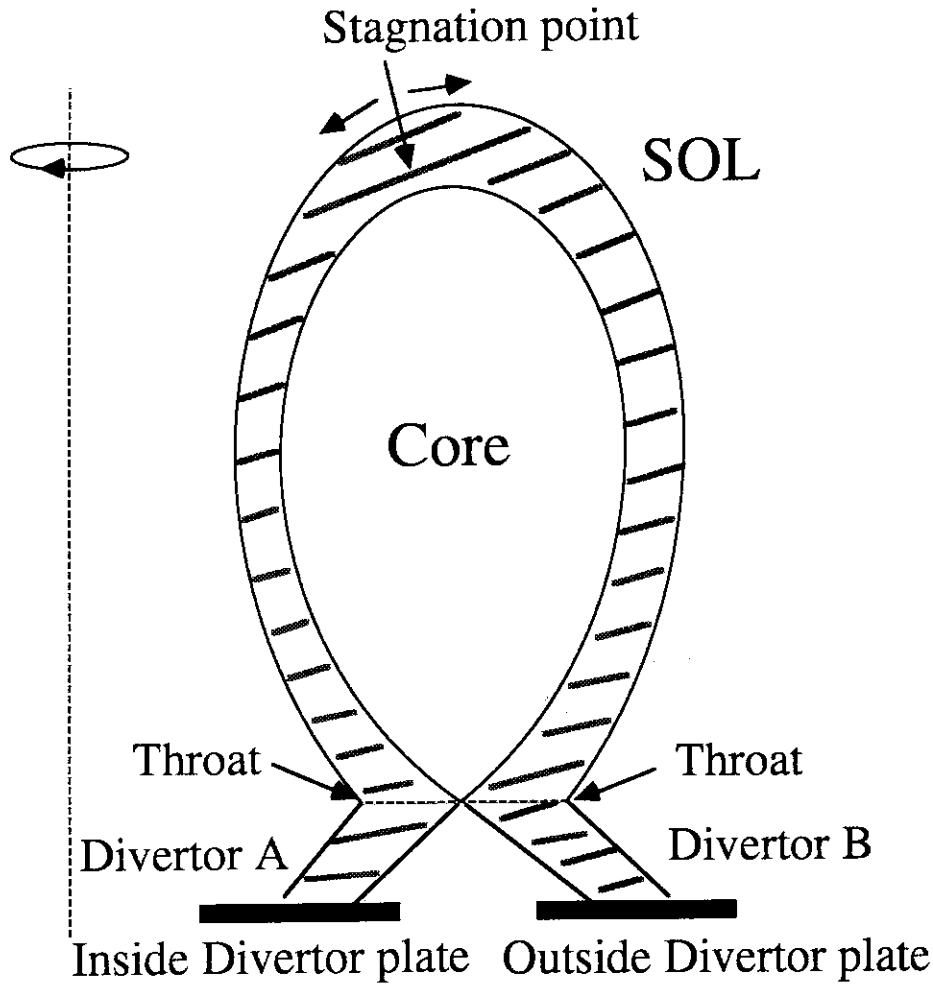

Fig.1 Scrape-off layer and divertor plasmas
in a single-null divertor tokamak

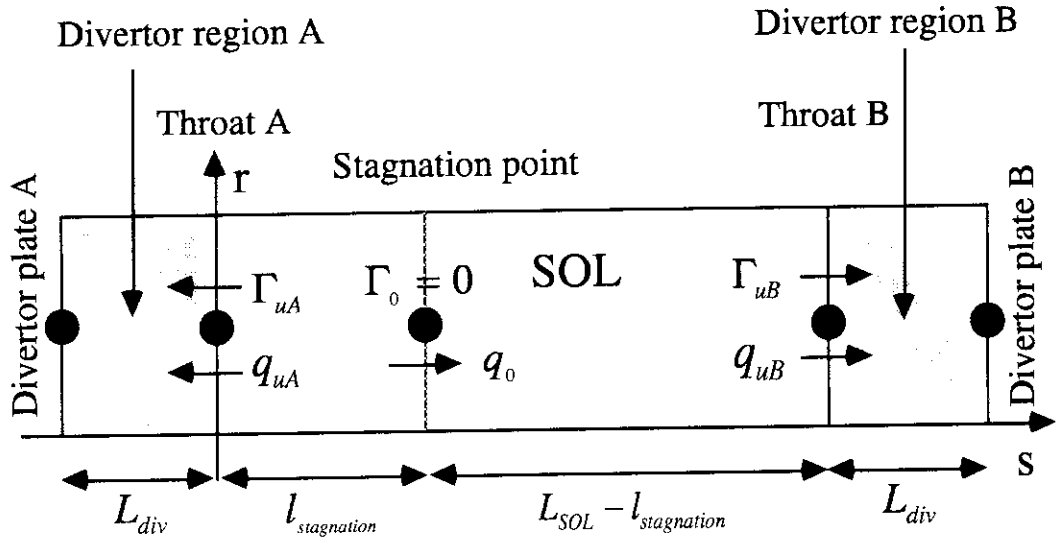

Fig.2 Five-point model

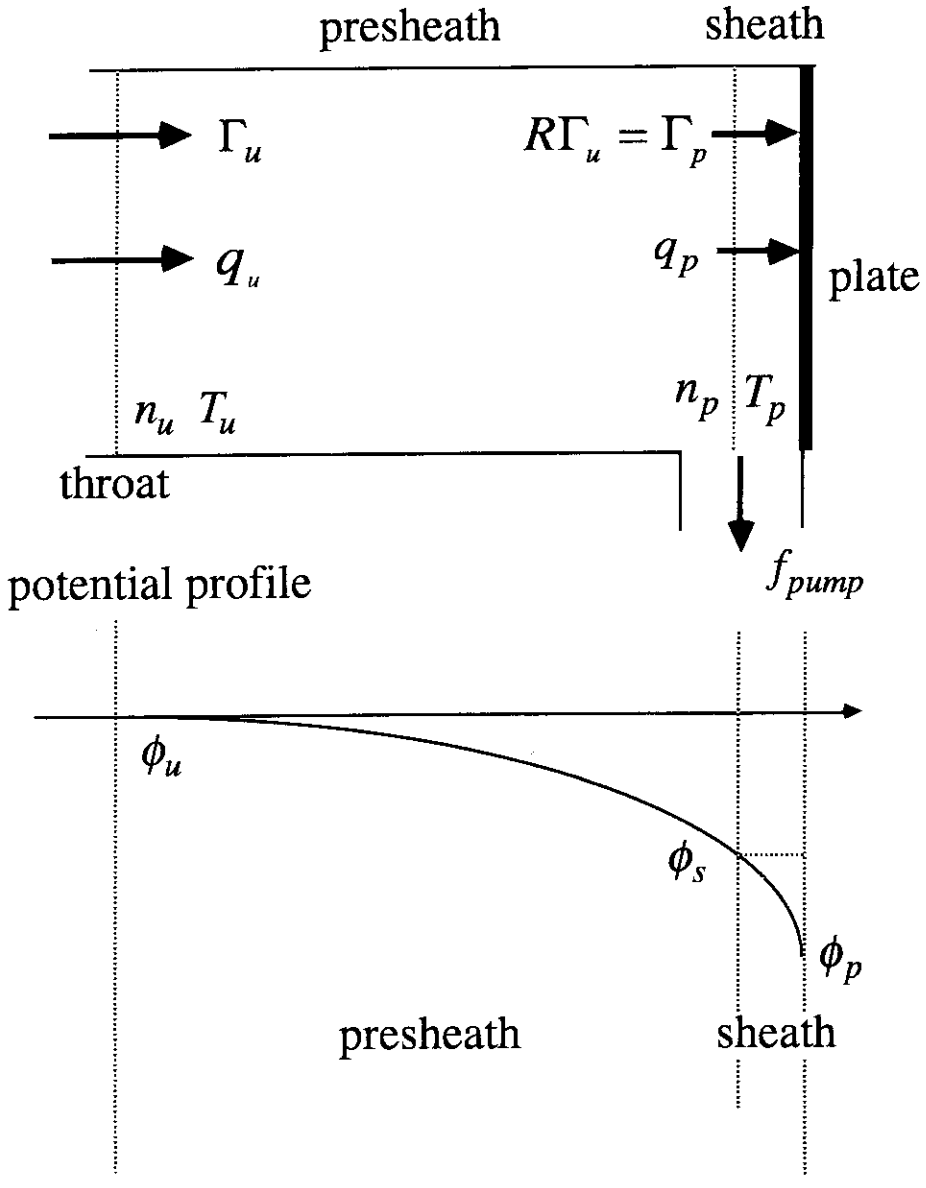

Fig.3 Divertor model

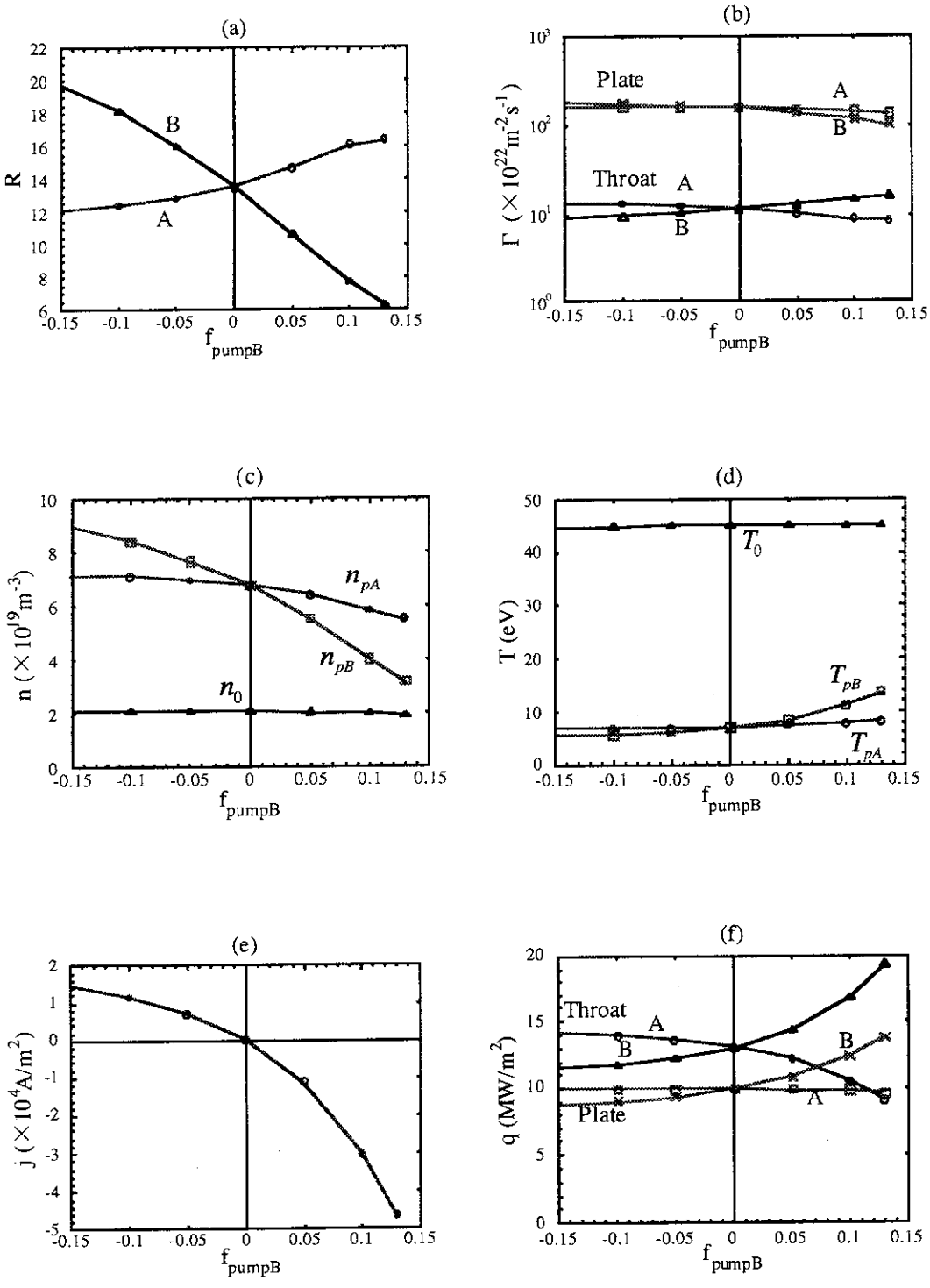

Fig.4 Gas pumping/puffing asymmetry. Gas pumping/puffing at outside divertor B. (a) flux amplification factor, (b) particle flux, (c) plasma density, (d) plasma temperature, (e) SOL current, and (f) heat flux.

(a) Gas pumping

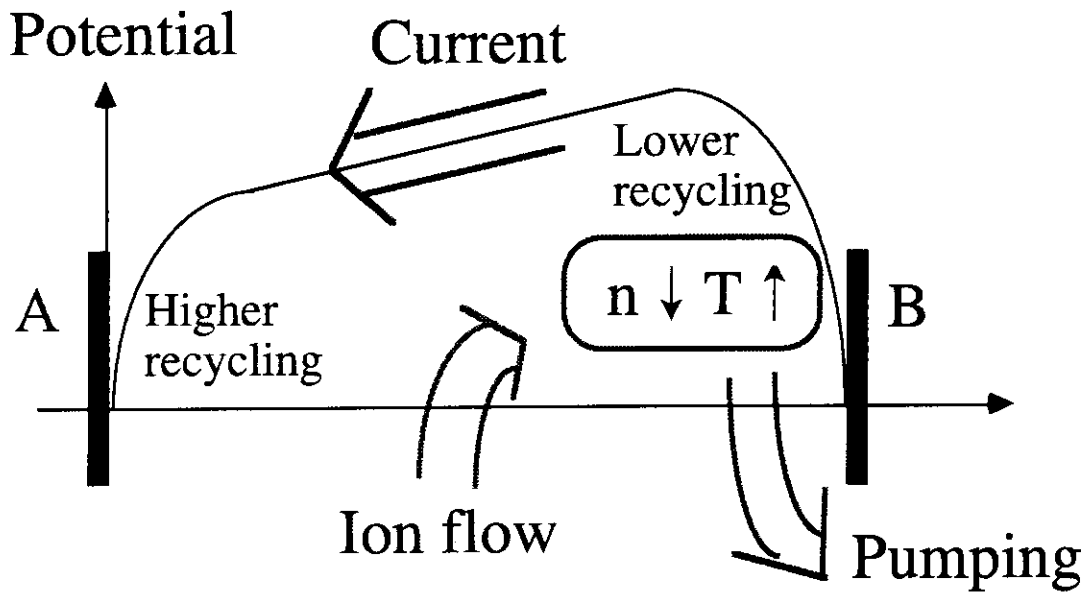

(b) Gas puffing

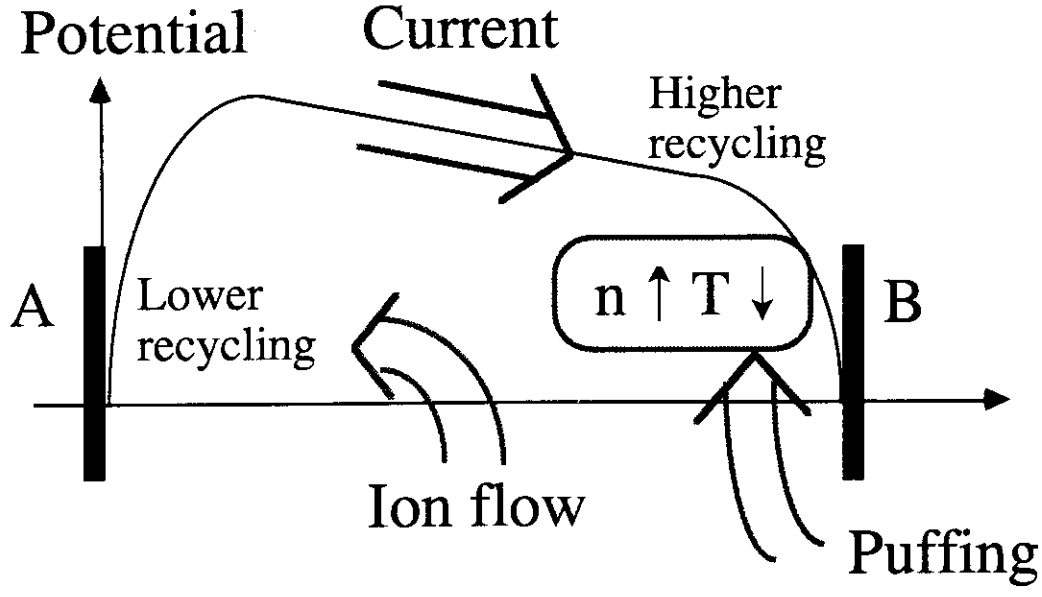

Fig.5 Illustrations of the results of gas pumping/puffing asymmetry.

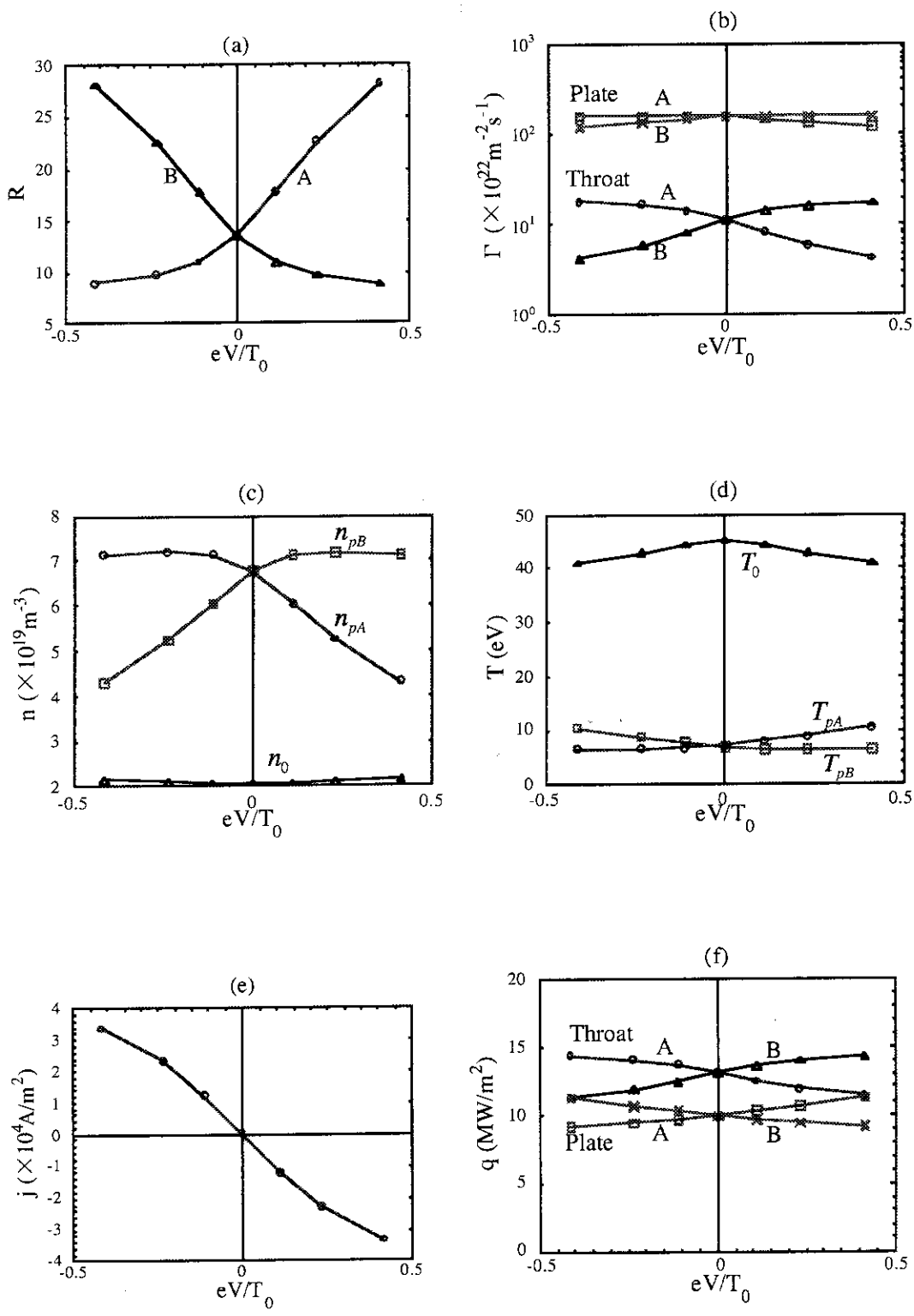

Fig.6 Biasing asymmetry. (a) flux amplification factor, (b) particle flux, (c) plasma density, (d) plasma temperature, (e) SOL current, and (f) heat flux.

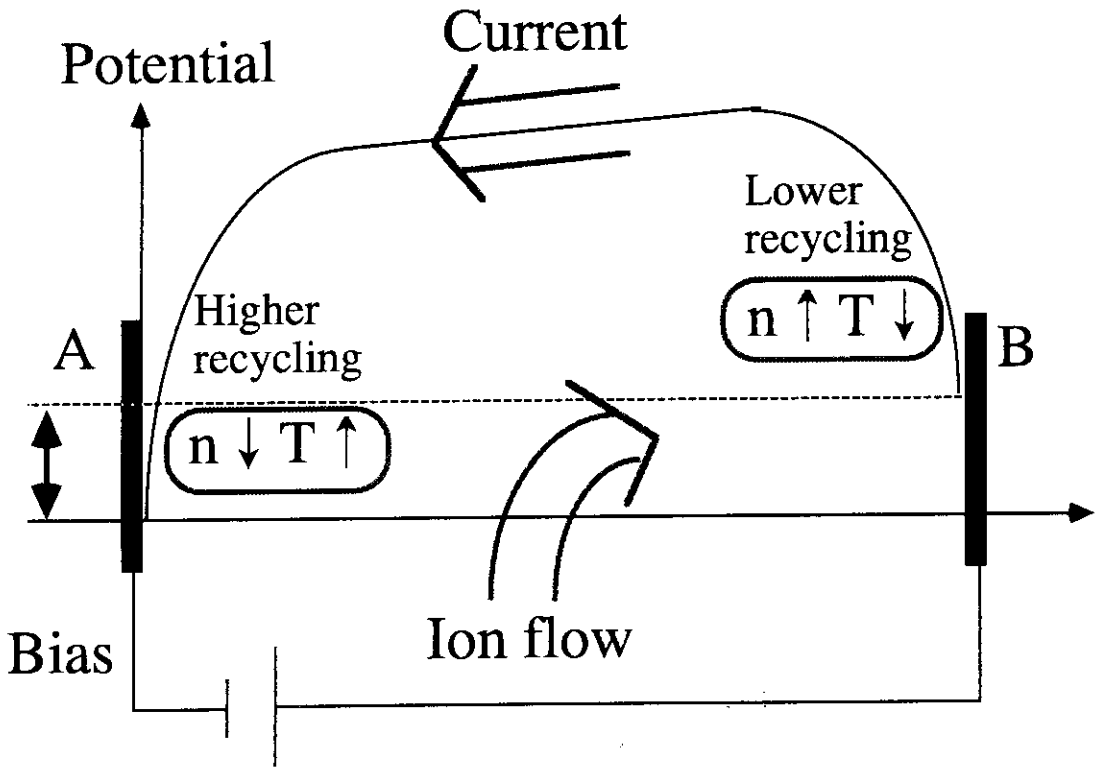

Fig.7 Illustrations of the results of biasing asymmetry

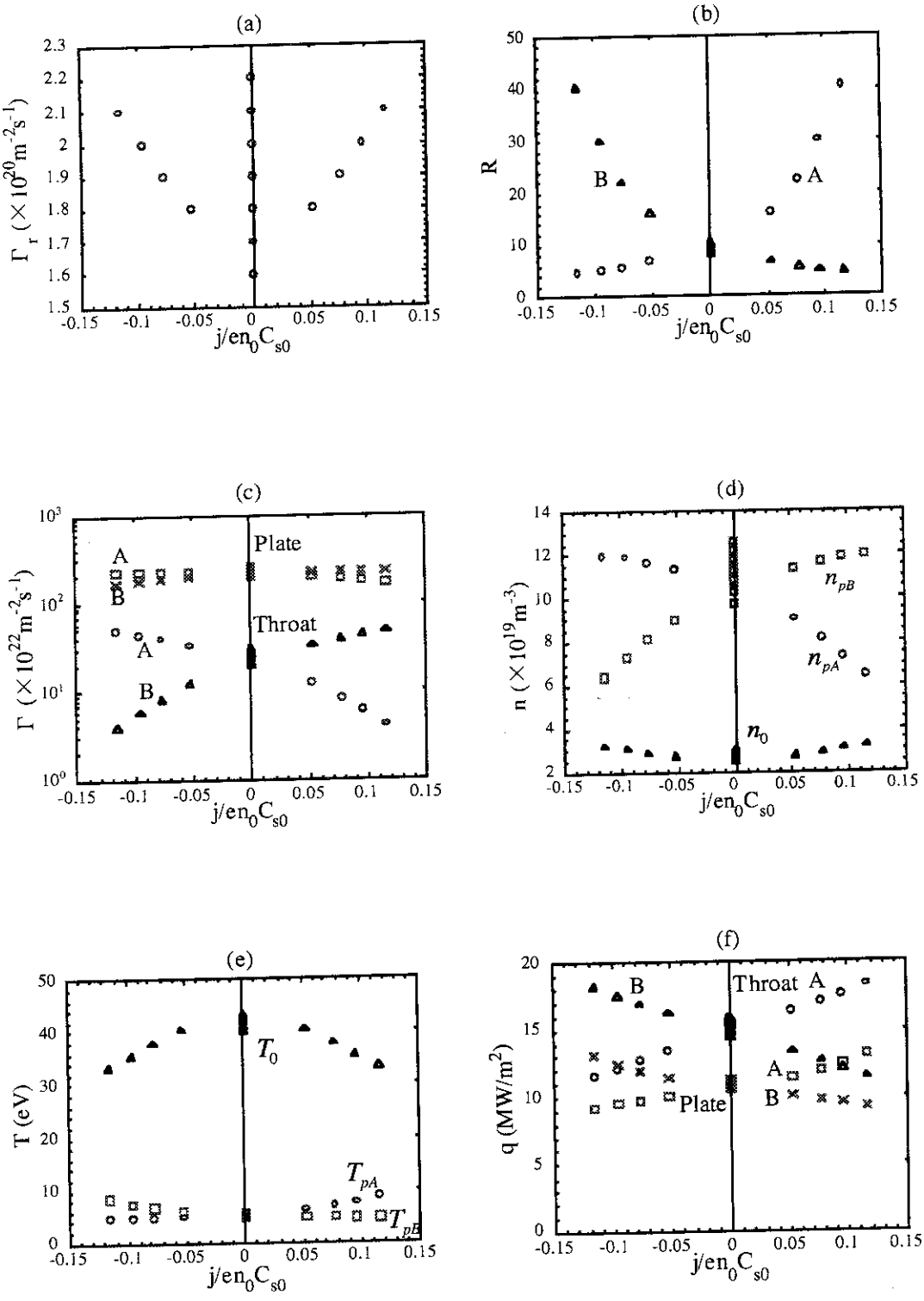

Fig.8 Current asymmetry without gas pumping/puffing and biasing. (a) ion flux from core plasma, (b) flux amplification factor, (c) particle flux, (d) plasma density, (e) plasma temperature, and (f) heat flux.

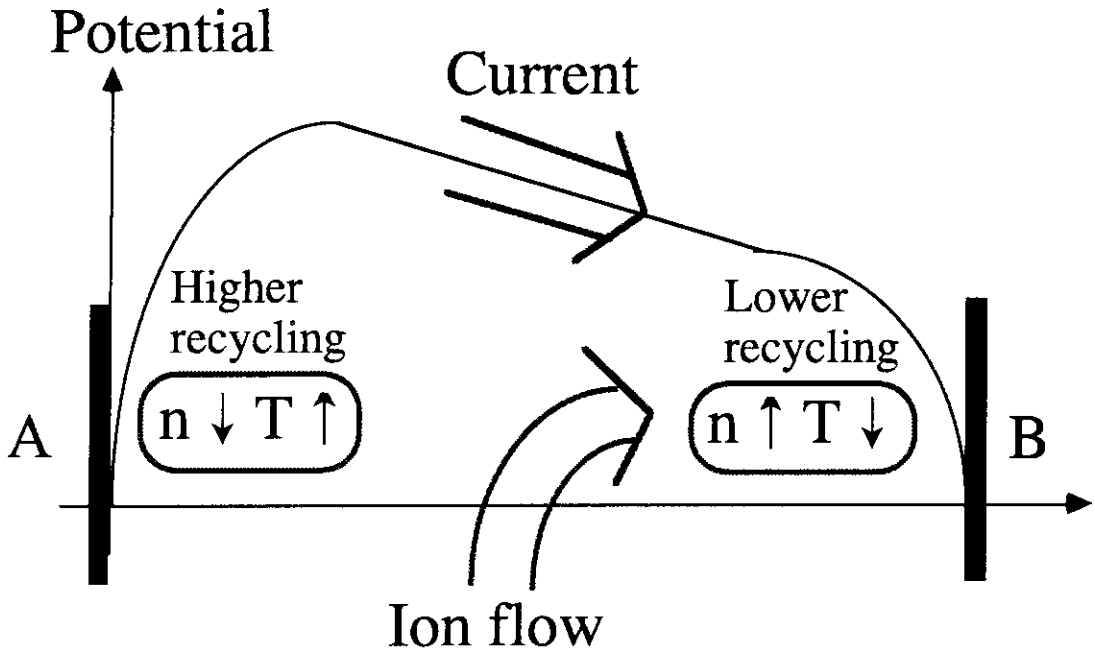

Fig.9 Illustrations of the results of current asymmetry

Appendix

A.1 The method to solve the five-point model

Values of 8 parameters, Γ_r, q_r, $D_\perp$, $\chi_\perp$, f_{pumpA}, f_{pumpB}, ϕ_{pA}, and ϕ_{pB}, are given. At first we put arbitrary values for four unknown variables, the density at stagnation point n_0, the temperature at stagnation point T_0, the SOL current j, and the stagnation position $l_{stagnation}$. By using above 12 values, particle and energy source terms in the SOL are rewritten from Eqs.(7)-(10),

$$S_{SOL} = \frac{\Gamma_r^2}{D_\perp n_0} \tag{A1}$$

$$W_{SOL} = \frac{q_r^2}{\chi_\perp n_0 T_0} + \frac{q_r \Gamma_r}{D_\perp n_0}. \tag{A2}$$

Input particle fluxes to each divertor two-point model are given by Eqs.(11) and (14) as follows.

$$\Gamma_{uA} = S_{SOL} l_{stagnation} \tag{A3}$$

$$\Gamma_{uB} = S_{SOL}\left(L_{SOL} - l_{stagnation}\right) \tag{A4}$$

Given above input parameters, Γ_{uA}, $-j$, n_0, T_0, f_{pumpA}, and ϕ_{pA}, to the divertor A model, we obtain values of variables at the throat, T_{pA}, ϕ_{uA}, and q_{uA}. In the same way, given input parameters, Γ_{uB}, j, n_0, T_0, f_{pumpB}, and ϕ_{pB}, to the divertor B model, we obtain T_{pB}, ϕ_{uB}, and q_{uB}. These procedures are described in A.1.1.

From the model, we derive the following equations.

$$G_1\left(n_0, T_0, j, l_{stagnation}\right) = j + \frac{\sigma_0 T_0^{3/2}}{L_{SOL}}\left(\phi_{uB} - \phi_{uA}\right) = 0 \tag{A5}$$

$$G_2\left(n_0, T_0, j, l_{stagnation}\right) = q_{uB} + q_{uA} - W_{SOL} L_{SOL} + j\left(\phi_{uB} - \phi_{uA}\right) = 0 \tag{A6}$$

$$G_3\left(n_0, T_0, j, l_{stagnation}\right) = q_{uA} + \frac{2}{7}\kappa_0 \frac{T_{pA}^{7/2} - T_0^{7/2}}{l_{stagnation} + L_{div}} - \left(\frac{5}{2} + \alpha\right)\frac{j}{e} T_0 - 5 T_0 \Gamma_{uA} = 0 \tag{A7}$$

$$G_4\left(n_0, T_0, j, l_{stagnation}\right) = q_{uB} + \frac{2}{7}\kappa_0 \frac{T_{pB}^{7/2} - T_0^{7/2}}{L_{SOL} - l_{stagnation} + L_{div}} + \left(\frac{5}{2} + \alpha\right)\frac{j}{e}T_0 - 5T_0\Gamma_{uB} = 0 \tag{A8}$$

We evaluate whether above guess values of n_0, T_0, j, and $l_{stagnation}$, satisfy these nonlinear equations (A5-8) or not. When these functions G_1, G_2, G_3, and G_4, approach to zero within quite small errors, the guess values are proper. The nonlinear equations are solved by a numerical method described in A.1.2. If the solutions of n_0, T_0, j, and $l_{stagnation}$, are found, other unknown values are also found to each solutions by using the following equations.

$$\lambda_n = \frac{D_\perp n_0}{\Gamma_r} \tag{A9}$$

$$\lambda_T = \frac{\chi_\perp n_0 T_0}{q_r} \tag{A10}$$

$$\phi_0 = \frac{\phi_{uB} + \phi_{uA}}{2} + \frac{j}{\sigma_0 T_0^{1.5}}\left(\frac{L_{SOL}}{2} - l_{stagnation}\right) \tag{A11}$$

$$q_0 = \frac{q_{uB} - q_{uA}}{2} + j\frac{\phi_{uB} + \phi_{uA} - 2\phi_0}{2} - W_{SOL}\left(\frac{L_{SOL}}{2} - l_{stagnation}\right) \tag{A12}$$

A.1.1 Divertor two-point model

Values of 6 parameters, Γ_u, j, n_0, T_0, f_{pump}, and ϕ_p, are given as input parameters to the divertor model. At first we put arbitrary value for the plate temperature T_p. From Eq.(32), the plate density is written by given parameters as follows,

$$n_p = \frac{n_0 T_0}{2T_p}. \tag{A13}$$

Particle flux at plate is written by Eq.(27).

$$\Gamma_p = n_p\sqrt{\frac{2T_p}{m}} = \frac{n_0 T_0}{\sqrt{2mT_p}} \tag{A14}$$

Flux amplification factor R is defined by,

$$R=\frac{\Gamma_p}{\Gamma_u}=\frac{n_0T_0}{\sqrt{2mT_p}\Gamma_u}. \tag{A15}$$

Particle balance equation is rewritten from Eqs.(22) and (26) as follows.

$$R-1=R\eta \tag{A16}$$

$$\begin{cases}\eta=\left(1-f_{pump}\right)\left\{1-\exp\left(-\dfrac{\theta L_{div}}{\lambda}\right)\right\}\\ \lambda=\dfrac{\upsilon_0}{n_p\langle\sigma\upsilon\rangle_{T_p}}=\dfrac{2T_p\sqrt{T_p/m_0}}{n_0T_0\langle\sigma\upsilon\rangle_{T_p}}\end{cases} \tag{A17}$$

From these equations, a nonlinear equation of T_p is obtained.

$$F\left(T_p\right)=1-R(1-\eta)=1-\frac{n_0T_0}{\sqrt{2mT_p}\Gamma_u}\left[1-\left(1-f_{pump}\right)\left\{1-\exp\left(-\frac{\theta L_{div}n_0T_0\langle\sigma\upsilon\rangle_{T_p}}{2T_p\sqrt{T_p/m_0}}\right)\right\}\right]=0 \tag{A18}$$

When the function $F\left(T_p\right)$ approaches to zero within a small errors, the guess value of T_p is proper. The nonlinear equation is solved by a numerical method. The equation has three solutions. The lowest T_p corresponds to the high recycling, the highest T_p to the low recycling, and the middle T_p to the unstable states. We choose the high recycling solution among them. When a solution of T_p is found, other unknown values are easily obtained by using following equations.

$$\hat{j}=\frac{j}{e\Gamma_p} \tag{A19}$$

$$\phi_s=\phi_p+\frac{T_p}{e}\left\{\beta-\ln\left(1-\hat{j}\right)\right\} \tag{A20}$$

$$\gamma=\gamma_0-2\hat{j}-\ln\left(1-\hat{j}\right) \tag{A21}$$

$$q_p=\gamma\Gamma_pT_p \tag{A22}$$

$$\phi_u=\phi_s+\frac{L_{div}}{\sigma_0}jT_0^{-\frac{3}{2}}-\frac{\alpha}{e}\left(T_p-T_0\right)+\frac{T_0}{2e} \tag{A23}$$

$$q_u=q_p-j\left(\phi_u-\phi_p\right)+\Delta E\Gamma_p\eta \tag{A24}$$

A.1.2 The numerical method

We consider a function F of a variable x. The function equals zero at several values of the variable. In order to find the roots for F=0, we use a numerical method explained as follows.

Within a domain of x between a and b to be examined in Fig.A1, we divide this domain into many regions small enough that there is less or only one root in a region. Comparing signs of the function at both edges of each region, we can find a root in the region. When signs are different, there is a root in the region. On the other hand, when signs are the same, there is no root in the region. This method makes a loop of searching the regions which include the roots of the variable. After the existence of the root is confirmed in all regions, the exact value of the root is searched within quite small errors using the method of bisection. The method described above costs many calculations in computer but is simplest way to find multiple roots exactly.

Additionally the method can be also applied easily the case of multiple equations ($F_1(\mathbf{x})=0 \sim F_n(\mathbf{x})=0$) of the same number of variables ($\mathbf{x} = (x_1 \sim x_n)$). To find roots of one variable needs one equation. Each equation makes a loop of searching for the roots of the variable. These loops make a combination as seen in Fig.A2. The case of two coupled equations are explained as follows.

1) A domain of x_2 is divided to regions whose edge values of x_2 are expressed by $x_{2,i}$ (i=1,2, ~).

2) $x_1(x_{2,i})$ which satisfy $F_1(x_1(x_{2,i}),x_{2,i})=0$ are found by using above numerical method.

3) Signs between $F_2(x_1(x_{2,i}),x_{2,i})$ and $F_2(x_1(x_{2,i+1}),x_{2,i+1})$ are comparing. When their signs are opposite, there is a root of x_2 in the region $x_{2,i} < x_2 < x_{2,i+1}$.

4) The root of x_2 in this region is searched for by the method of bisection, with calculating the x_1 loop.

This numerical method can be easily applied to the case of many variables.

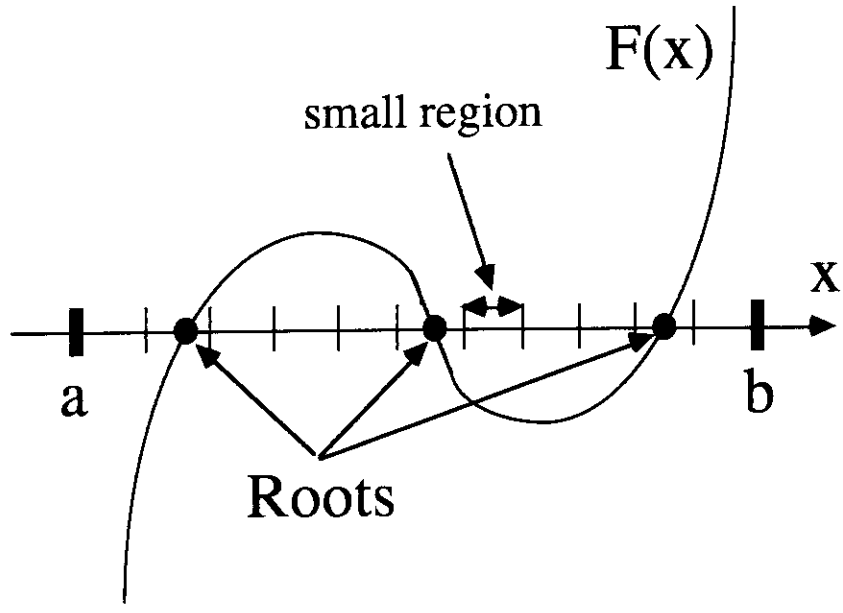

Fig.A1 A function F with a variable x

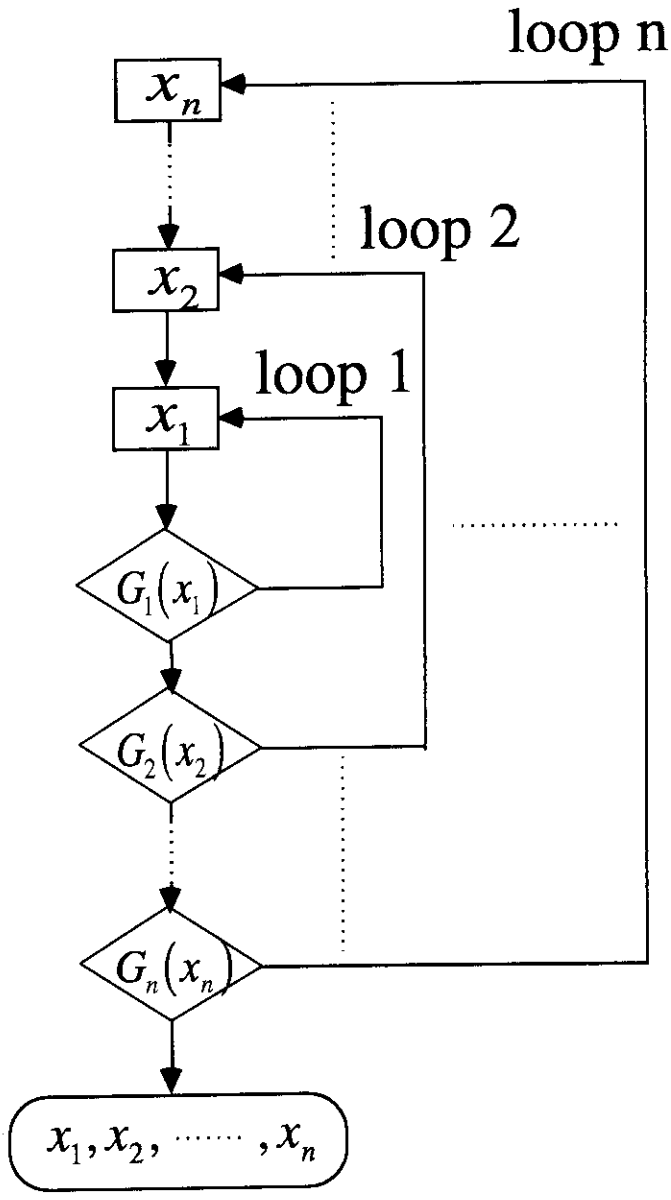

Fig.A2 Numerical method of multiple equations